Enabling Low Sidelobe Secret Multicast Transmission for mmWave Communication: An Integrated Oblique Projection Approach

Miao He, *Student Member, IEEE,* Jianbing Ni, *Senior Member, IEEE,* Meng Li, *Member, IEEE,* Alessandro Brighente, and Mauro Conti, *Fellow, IEEE*

***Abstract*—millimeter-wave (mmWave) is one of the most promising technologies for 5G and beyond networks. Indeed, thanks to its higher available spectrum, it allows operators to serve a larger number of users. Up to now, data transmission in mmWave communication has been protected with optimized secrecy for a single receiver, but the secrecy of multicast transmission has not been achieved on the physical layer. It is hence fundamental to design a secrecy-preserving scheme that concurrently allows to protect the communication of multiple users.**

In this paper, we propose a low sidelobe secret multicast transmission scheme in mmWave communication based on physical layer security techniques. Specifically, considering the requirement of multiple-beam with the channel knowledge of all target users, we design a primary transmitting weight vector of the base station to achieve a low sidelobe transmitting pattern. Also, we develop a transformation matrix from the oblique projection matrices of all the target users' channel vectors. In each symbol period, the transmitting weight vector of the base station is updated by performing a linear transformation on the primary weight vector with the transformation matrix. Consequently, the expected symbols for target users at the desired directions can be synthesized under multicast directional modulation transmission without jeopardizing the low sidelobe transmitting pattern. Meanwhile, the eavesdroppers cannot acquire any useful information from the received signals because of the artificial noise, which brings the randomness to the transformation matrix at the symbol rate. Via numerical simulation, we demonstrate that our proposed scheme achieves outstanding communication performance for the target users with the low sidelobe pattern, while keeping high symbol error rate on the undesired directions.

***Index Terms*—Physical layer security, secure mmWave communication, low sidelobe pattern, oblique projection**

I. Introduction

Due to high carrier frequency and small wavelength, millimeter-wave (mmWave) wireless communication has many advantages over low-frequency communication, such as narrow antenna beam [1], wide transmission spectrum band [2], low transmission latency [3], and comparable coverage with high data rates [4]. Various communication systems and standards adopted mmWave wireless communication techniques, including but not limited to the 5G systems and satellite communications. Furthermore, they are also expected to be applied in the 6G communication systems based on Cybertwin [5] or other novel network architectures, supporting future growing network applications in the Internet of Everything [6] and military networks [7].

Although mmWave communication supports many advanced applications, the data security issue has become the bottleneck. The open nature of the wireless medium makes mmWave communication vulnerable to eavesdroppers [8], [9]. In addition to data encryption at the application or network layer that relies on cryptographic keys with secure key management, Physical Layer Security (PLS) [10] is another effective technique to achieve secret communication at the physical layer without complex key management schemes [11], [12]. The fundamental principle of PLS is to exploit the inherent randomness of noise and communication channels to limit the amount of information that can be extracted at the bit level by unauthorized receivers [13]. Typical PLS approaches for mmWave communication secrecy include Directional Modulation (DM) and Artificial Noise (AN). In DM, the desired constellations can be synthesized at the target users' directions by designing appropriate weight vectors of the transmitting antennas. Meanwhile, the randomness can be added to the signals in the undesired directions at symbol rate. Thus, the eavesdroppers can hardly demodulate the received signals to extract the information for the target user [14], [15]. AN is added to the signal transmitted by a legitimate user to protect the carried information from non-legitimate receivers [16]. By adopting well-designed weight vectors of the transmitting antenna, the transmitter adds the noise in the orthogonal subspace of the legitimate channel to ensure only the eavesdroppers' channels are impaired [17].

Currently, most of the DM or AN based PLS schemes [18]–[20] only provide secrecy protection for a single target user in mmWave communication. Protecting the multicast mmWave communication still represents an open problem. This is fundamental, as multicast is an efficient and important communication mode in data collecting scenarios [21], such as the Internet of Things (IoT) for environment monitoring [22], e-health [23], and smart home [24]. Besides, the existing mmWave PLS schemes [18]–[20] have not considered the communication performance optimization for the target user. Several secret transmission schemes aiming at multiple target user communication scenarios have been developed [25], [26],

M. He and J. Ni are with the Department of Electrical and Computer Engineering and Ingenuity Labs Research Institute, Queen's University, Kingston, Ontario, Canada K7L 3N6. Email: {19mh48, jianbing.ni}@queensu.ca.

M. Li is with the School of Computer Science and Information Engineering, Hefei University of Technology, Hefei, 230601, China. Email: mengli@hfut.edu.cn.

A. Brighente and M. Conti are with the Department of Mathematics and HIT Research Center, University of Padova, 35131, Padua, Italy. Email: {alessandro.brighente, mauro.conti}@unipd.it.

but they do not have the low sidelobe transmitting pattern, which optimizes the transmitting power to focus on the target users. In fact, the low sidelobe transmission can improve the multicast communication performances by improving the target users' Signal-to-Noise Ratios (SNRs). Meanwhile, it allows to reduce the power transmitted to the eavesdroppers' directions.. Therefore, it is promising to have the low sidelobe transmitting pattern in PLS communication systems, especially under the multicast scenarios.

In this paper, we propose a low sidelobe secret multicast transmission scheme for securing the multicast communication between a Base Station (BS) and multiple target users. We assume a single-path channel in a mmWave communication system. Directly achieving secret low sidelobe multicast communication through optimization involves executing optimization at the symbol rate, which results in high computational cost. An alternative way is to securely add transmitting symbols to the pre-optimized low sidelobe transmitting pattern at the symbol rate with PLS techniques. However, the low sidelobe transmitting pattern may be deteriorated by the secrecy protection measures. To solve these problems, we exploit the integrated oblique projection approach based on the joint of DM transmission and AN superposition to protect the optimized multicast communication, without deteriorating its original low sidelobe transmitting pattern. First, knowing channel vectors of the target users, we obtain a primary transmitting weight vector of the BS through optimization with the constraint that the array transmitting pattern is designed to be multiple-beam and low sidelobes [27]. Since each pattern mainlobe is devised toward one target user direction in order to improve its receiving SNR, we achieve optimized multicast communication for the target users based on the primary transmitting weight vector. Second, with the aid of the vector oblique projection of the target users' channel vectors [28], [29], we construct a transformation matrix. The transmitting weight vector of the BS antenna array can be computed by performing a linear transformation on the obtained primary weight vector by using the obtained transformation matrix. By updating the parameters corresponding to the target users' directions at the symbol rate, we synthesize the desired constellation of each target user at each symbol time instant without jeopardizing the optimized low sidelobe transmitting pattern. Third, we add a random parameter in the operation of linear transformation, so as to remove the needed additional hardware. This randomness only affects the constellations at the undesired directions.

Our contributions can be summarized as follows.

- We improve the state-of-the-art on PLS communication secrecy by dealing for the first time the multicast communication scenario.
- We propose a low complexity solution that exploits the combination of a pre-optimized low sidleobe transmit pattern and oblique projection to avoid impairing the computational efficiency of the transmitter.
- Via thorough numerical simulation, we show the effectiveness of our novel scheme in achieving both secrecy and communication efficiency.

The unique features of our new PLS transmission scheme can be summarized as follows:

1) Our new scheme protects the secrecy of multicast mmWave communication, by jointly utilizing the multicast DM transmission and the AN superposition.
2) Our new scheme has the optimized low sidelobe transmitting pattern on the multi-beams. We propose an integrated oblique projection approach to achieve the desired multiuser constellation synthesis and the AN superposition. The low sidelobe transmitting pattern obtained from the optimization performed before adding secrecy protections is not jeopardized.
3) Our new scheme is affordable for the practical implementation due to its low computational complexity in weight vector update. The weight vector is updated at the lightweight cost of addition, multiplication, and linear transformation in each symbol period. No additional hardware is needed to support the weight vector update.

The remainder of the paper is organized as follows. We review the related work in Section II, present the system model and formulate the problem in Section III, and introduce the oblique projection in Section IV. In Section V, we proposed our secure multicast transmission scheme, followed by the performance evaluation in Section VI. Finally, we present the simulation results in Section VII and draw the conclusion in Section VIII.

II. Related Work

The typical PLS approaches for mmWave communication secrecy are mainly based on DM and AN. Daly *et al.* [14], [15] firstly introduced DM to achieve secrete wireless communication. A genetic algorithm is applied to find suitable sets of phase shifts with the goal of minimizing a cost function that is the sum of the square magnitudes between the desired constellation points and the transmitted points on a constellation diagram. Valliappan *et al.* [18] proposed an Antenna Subset Modulation (ASM) scheme for mmWave communication. In ASM, the randomness is added to the constellations at undesired directions by selecting different subsets of the transmitting array antennas at a symbol rate with Radio Frequency (RF) on-off switches. A modified ASM transmission architecture called Switched Phase Array (SPA) [19] is proposed by turning off one RF switch at the symbol rate. Recently, Hong *et al.* proposed a scheme [20] consisting of a conventional phased-array architecture based on programmable power amplifiers used to change the amplitudes of antenna element weights. Instead of utilizing RF on-off switches, programmable power amplifiers are used on the antennas to achieve scrambled constellations at undesired directions. Unfortunately, these mentioned DM schemes [18]–[20] cannot support secret multicast communication with low sidelobe.

The concept of AN is introduced by Goel and Negi [16], where the artificial noise is added to the signal carrying information in order to protect the confidentiality of the carried information in transmission. The randomness brought by the AN is designed to be effective in the orthogonal

subspace of the desired users' channels [17], [30], so that only the eavesdroppers' channels are contaminated by the artificial noise. Shu *et al.* [26] proposed an AN-aided secure scheme in a multicast scenario by adopting proper precoding vector for each group of target users. The precoding vector can be obtained by maximizing the receiving power of each target group subject to the orthogonal constraint. In addition, the AN is projected to the null space of all target users' steering vectors. Recently, Xu *et al.* [31] proposed a secure communication scheme for a mmWave system for the receivers equipped with multiple receiving antennas. The transmitting symbol is precoded onto the dominant angle components of the target user's sparse channel through a limited number of RF chains, while AN is broadcast over other undesired directions to interfere the eavesdroppers. However, the aforementioned AN schemes need additional RF chains or additional computational cost for AN generation.

III. System Model and Problem Formulation

In this section, we present the system model in which a BS transmits messages to multiple target users through single-path mmWave channels, and formulate the problem of secret multicast transmission based on PLS. The relevant symbol notations in the system model are defined as follows: the matrices and vectors are denoted as the bold upper case letters (e.g., $\mathbf{A}$) and the bold lower case letters (e.g., $\mathbf{h}$). $|\cdot|$ indicates the absolute value. $j \triangleq \sqrt{-1}$. $(\cdot)^{\mathrm{T}}$ and $(\cdot)^{\mathrm{H}}$ denote the transpose and the Hermitian transpose, respectively. $\mathbb{C}$ and $\mathbb{R}$ denote the sets of complex numbers and the sets of real numbers, respectively. $\mathcal{R}(\cdot)$ returns the column space of the input matrix. $\mathcal{R}^{\perp}(\cdot)$ is the orthogonal complementary space of $\mathcal{R}(\cdot)$. $\mathcal{CN}\left(\mu, \sigma^2\right)$ represents the circularly symmetric complex Gaussian distribution with mean μ and variance σ^2.

A. System Model

In the system model, the downlink mmWave wireless communication system includes one BS and multiple target users, as illustrated in Fig. 1. The BS is equipped with an N-element Uniform Linear Array (ULA) with the element space $d = \lambda/2$, where λ is the wave length of the mmWave signal.

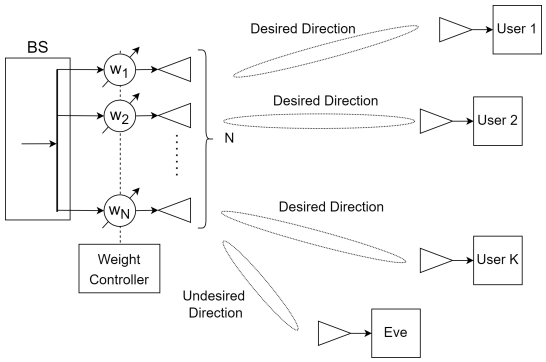

Fig. 1. The downlink mmWave wireless communication system with an N-element ULA and K target users under single-path mmWave channels.

We assume that the system model has K target users in total, where $K \leq N$. For mmWave wireless communication, due to the highly directional nature of the mmWave, the Line-of-Sight (LoS) path usually dominates over the multiple paths. Thus, the single-path mmWave channel is commonly assumed [32]. The k^{th} target user channel vector $\mathbf{h}_k$ can be expressed as

$$\mathbf{h}_k = \mathbf{a}(\theta_k) = \left[1, e^{j\mu_k}, e^{j2\mu_k}, \cdots, e^{j(N-1)\mu_k}\right]^T, \quad (1)$$

where $\mathbf{a}(\theta_k)$ is the array steering vector for the k^{th} target user, $\mu_k = (2\pi d/\lambda)\sin\theta_k$, θ_k is the Angle of Depature (AoD). Here $\mathbf{h}_k = \mathbf{a}(\theta_k)$ is assumed to be known to the BS.

The transmitting symbol to the k^{th} user at time instant t (the t^{th} symbol period) is denoted as s_k. With the channel vector $\mathbf{h}_k = \mathbf{a}(\theta_k)$, the BS transmitting weight vector $\mathbf{w}$ should satisfy

$$\mathbf{a}^H(\theta_k)\mathbf{w} = \gamma_k s_k, \quad k = 1, 2, \cdots K, \quad (2)$$

$$\mathbf{w} = [w_1, w_2, \cdots, w_N]^T, \quad (3)$$

where γ_k is the scaling factor related to the channel gain or the received SNR for the k^{th} target user. The transmitting symbol s_k can have M symbol states. For example, if the modulation is Binary Phase Shift Keying (BPSK), $M = 2$, the phase of s_k can be 0 or π. Similarly, if the modulation is Quadratic Phase Shift Keying (QPSK), $M = 4$, the phase of s_k can be $\pi/4$, $3\pi/4$, $5\pi/4$, or $7\pi/4$. In each symbol time instant, the BS should synthesize the symbol s_k of the k^{th} target user with the gain γ_k by designing an appropriate time-varying transmitting weight vector $\mathbf{w}$. With the multiuser assumption, in order to obtain a common transmitting weight vector satisfying all equations in (2) at each time instant, the transmitting weight vector $\mathbf{w}$ is not constrained to be a constant modulus. Instead, the elements in the weight vector can be any complex values. Both the amplitude and phase of each element in the weight vector $\mathbf{w}$ are changeable.

B. Problem Formulation

To achieve multicast transmission, a common transmitting weight vector $\mathbf{w}$ is obtained by directly solving the following equations

$$\begin{cases} \mathbf{w}^H\mathbf{a}(\theta_1) = \gamma_1 s_1, \\ \mathbf{w}^H\mathbf{a}(\theta_2) = \gamma_2 s_2, \\ \vdots \\ \mathbf{w}^H\mathbf{a}(\theta_K) = \gamma_K s_K, \end{cases} \quad (4)$$

where $[s_1, s_1, \cdots s_K]$ is a given symbol set transmitted to the K target users, and $K \leq N$.

Unfortunately, the transmitting weight vector obtained in Eqn. (4) cannot guarantee the communication secrecy or provide the low sidelobe transmitting pattern, since significant transmitting power may be leaked at the undesired directions. In a secrecy-preserving wireless communication system, to improve the communication secrecy, it is expected that the antenna radiates as little power as possible to the undesired directions for the purpose of ensuring reliable information transmission to the target users, so that the eavesdroppers cannot efficiently obtain the information from the received weak signal.

To have low sidelobe multicast transmission, the pattern synthesis can be formulated as an optimization problem with the objective of finding the transmitting weight vector $\mathbf{w}$ that minimizes the sidelobe power $\left|\mathbf{w}^H\mathbf{a}(\theta)\right|$ within the angular range Θ, which is out of the angular width of the main lobe at each target direction. We hence formulate the problem as

$$\begin{aligned} &\underset{\mathbf{w}}{min}(\rho); \\ &subject\ to\ \mathbf{w}^H\mathbf{a}(\theta_k) = \gamma_k s_k, k = 1, 2, \cdots, K; \\ &\left|\mathbf{w}^H\mathbf{a}(\theta)\right| \leqslant \rho, \theta \in \Theta, \end{aligned} \tag{5}$$

where $\gamma_k s_k$ is the expected synthesized signal with gain γ_k for the k^{th} target user located at θ_k. No closed-form expression is available for the solution $\mathbf{w}$ to Eqn. (5), but the numerical solutions of the transmitting weight vector can be obtained from iterative optimization algorithms [33].

However, the approach derived from Eqn. (5) cannot achieve the efficient PLS protection for low sidelobe communication, since the information still can be recovered by eavesdroppers equipped with sufficiently sensitive radio receivers [14]. To increase secrecy, randomness should be added to the received weak signal at the undesired directions. Thus, the eavesdroppers face difficulties in demodulating the constellations from the deteriorated signals, even if they are equipped with highly sensitive radio receivers.

To protect the communication secrecy, DM transmission and AN superposition have been adopted to produce randomness to the received signals at the undesired directions. However, adopting these techniques to the multicast mmWave communication faces several challenges. First, the adopted DM transmission and AN superposition should support multiple target users. Second, the low sidelobe transmission pattern should be maintained after adding the secrecy protection measures, such as the DM and the AN. Third, the overall computational cost should be affordable for practical implementation. In contrast, the approach based on Eqn. (5), which achieves low sidelobe multicast communication through complex optimization operations in each symbol period. Specifically, the data transmission rate for the typical mmWave communication can be up to 2 Gbps [34]. For the QPSK modulation, the symbol rate is up to 1 GBd. The approach is not practical for implementation due to the extremely heavy burden of the optimization in Eqn. (5) at such high symbol rate.

IV. Preliminary: Oblique Projection

In this section, we briefly introduce the oblique projection and the matrix of oblique projection [28], [29].

Let us define $\mathbf{A} \in \mathbb{C}^{N\times(L_1+L_2)}$ as a full column rank matrix in the N dimensional space. The matrix can be partitioned as $\mathbf{A} = [\mathbf{A}_1, \mathbf{A}_2]$, where $\mathbf{A}_1 \in \mathbb{C}^{N\times L_1}$ and $\mathbf{A}_2 \in \mathbb{C}^{N\times L_2}$. The orthogonal projection vector $\mathbf{p} \in \mathbb{C}^{N\times 1}$ of any N dimensional vector $\mathbf{b} \in \mathbb{C}^{N\times 1}$ to the $(L_1 + L_2)$ dimensional subspace $\mathcal{R}(\mathbf{A})$ is given as

$$\mathbf{p} = \mathbf{P}_A\mathbf{b} = \left[\mathbf{A}(\mathbf{A}^H\mathbf{A})^{-1}\mathbf{A}^H\right]\mathbf{b}, \tag{6}$$

where the orthogonal projection matrix $\mathbf{P}_A$ is defined as $\mathbf{P}_A = \mathbf{A}(\mathbf{A}^H\mathbf{A})^{-1}\mathbf{A}^H$. The orthogonal projection matrix to the orthogonal complement space $\mathcal{R}^{\perp}(\mathbf{A})$ of $\mathcal{R}(\mathbf{A})$ is $\mathbf{P}_A^{\perp} = \mathbf{I} - \mathbf{P}_A$.

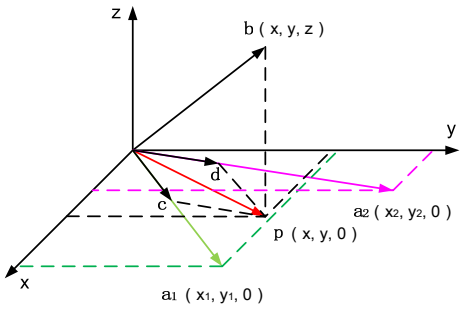

Fig. 2. The oblique projection. ($\mathbf{c} = \mathbf{E}_{1|2}\mathbf{b}$ and $\mathbf{d} = \mathbf{E}_{2|1}\mathbf{b}$ are the oblique projection vectors of $\mathbf{b} = [x, y, z]^T$ to the subspace $\mathcal{R}(\mathbf{a}_1)$ and $\mathcal{R}(\mathbf{a}_2)$, respectively.)

The orthogonal projection vector $\mathbf{p}$ can be further decomposed to the sum of a vector $\mathbf{c}$ in the subspace $\mathcal{R}(\mathbf{A}_1)$ and a vector $\mathbf{d}$ in the subspace $\mathcal{R}(\mathbf{A}_2)$ as,

$$\mathbf{p} = \mathbf{c} + \mathbf{d} = \mathbf{E}_{1|2}\mathbf{b} + \mathbf{E}_{2|1}\mathbf{b}. \tag{7}$$

The matrices $\mathbf{E}_{1|2}$ and $\mathbf{E}_{2|1}$ are termed as oblique projection matrix or oblique projector, thus,

$$\begin{aligned} \mathbf{E}_{1|2} &= \mathbf{A}_1(\mathbf{A}_1{}^H\mathbf{P}_2^{\perp}\mathbf{A}_1)^{-1}\mathbf{A}_1{}^H\mathbf{P}_2^{\perp}, \\ \mathbf{E}_{2|1} &= \mathbf{A}_2(\mathbf{A}_2{}^H\mathbf{P}_1^{\perp}\mathbf{A}_2)^{-1}\mathbf{A}_2{}^H\mathbf{P}_1^{\perp}, \end{aligned} \tag{8}$$

where $\mathbf{P}_1^{\perp} = \mathbf{I} - \mathbf{A}_1(\mathbf{A}_1^H\mathbf{A}_1)^{-1}\mathbf{A}_1^H$ and $\mathbf{P}_2^{\perp} = \mathbf{I} - \mathbf{A}_2(\mathbf{A}_2^H\mathbf{A}_2)^{-1}\mathbf{A}_2^H$ are the orthogonal projection matrices to the orthogonal complement spaces $\mathcal{R}^{\perp}(\mathbf{A}_1)$ and $\mathcal{R}^{\perp}(\mathbf{A}_2)$, respectively. In Eqn. (7), $\mathbf{c}$ can be taken as the projection vector of $\mathbf{b}$ onto the subspace $\mathcal{R}(\mathbf{A}_1)$ with projection matrix $\mathbf{E}_{1|2}$ along the direction parallel to the subspace $\mathcal{R}(\mathbf{A}_2)$. $\mathbf{d}$ can also be obtained likewise.

According to Eqn. (6) and Eqn. (7), the relationship between the orthogonal projection matrix and the oblique projection matrices is

$$\mathbf{P}_A = \mathbf{E}_{1|2} + \mathbf{E}_{2|1}. \tag{9}$$

In addition, it can be verified that the oblique projection matrices are idempotent but not Hermitian symmetric. They satisfy the following equations:

$$\begin{aligned} \mathbf{E}_{1|2}\mathbf{A}_1 &= \mathbf{A}_1, \quad \mathbf{E}_{1|2}\mathbf{A}_2 = \mathbf{0}, \\ \mathbf{E}_{2|1}\mathbf{A}_2 &= \mathbf{A}_2, \quad \mathbf{E}_{2|1}\mathbf{A}_1 = \mathbf{0}. \end{aligned} \tag{10}$$

To better understand the oblique projection, an example is illustrated in Fig. 2. In three dimensional space, there are two linearly independent vectors $\mathbf{a}_1 = [x_1, y_1, 0]^T$ and $\mathbf{a}_2 = [x_2, y_2, 0]^T$, by which the matrix $\mathbf{A} = [\mathbf{a}_1, \mathbf{a}_2]$ can be constructed. The subspace $\mathcal{R}(\mathbf{A})$ is the X-Y plane. The orthogonal projection vector $\mathbf{p}$ of vector $\mathbf{b} = [x, y, z]^T$ onto the subspace $\mathcal{R}(\mathbf{A})$ can be expressed as

$$\mathbf{p} = \mathbf{P}_A\mathbf{b} = \mathbf{A}(\mathbf{A}^H\mathbf{A})^{-1}\mathbf{A}^H\mathbf{b} = [x, y, 0]^T. \tag{11}$$

As illustrated in Fig. 2, the projection vector $\mathbf{p}$ can be decomposed into $\mathbf{c}$ and $\mathbf{d}$ with parallelogram rule, which is $\mathbf{p} = \mathbf{c} + \mathbf{d}$. $\mathbf{c} = \mathbf{E}_{1|2}\mathbf{b}$ and $\mathbf{d} = \mathbf{E}_{2|1}\mathbf{b}$ are the oblique projection vectors of $\mathbf{b} = [x, y, z]^T$ to the subspace $\mathcal{R}(\mathbf{a}_1)$ and $\mathcal{R}(\mathbf{a}_2)$, respectively.

More general, if $L \geq Q$, the full column rank matrix $\mathbf{A} \in \mathbb{C}^{N\times L}$ in N dimensional space can be partitioned as Q submatrices or subspaces in column as

$$\mathbf{A} = [\mathbf{A}_1, \mathbf{A}_2, \cdots, \mathbf{A}_Q], \tag{12}$$

where $\mathbf{A}_q \in \mathbb{C}^{N\times L_q}$, $q = 1, 2, \cdots, Q$ and $\sum_{q=1}^{Q} L_q = L$.

In Eqn. (12), if any $\mathbf{A}_q$ is considered as one submatrix, the other submatrices can be combined to constitute another submatrix $\mathbf{A}_{q-}$, which is described as

$$\mathbf{A}_{q-} = [\mathbf{A}_1, \cdots, \mathbf{A}_{q-1}, \mathbf{A}_{q+1}, \cdots, \mathbf{A}_Q] \in \mathbb{C}^{N\times(L-L_q)}. \tag{13}$$

Thus, Eqn. (12) can be rewritten as

$$\mathbf{A} = [\mathbf{A}_1, \mathbf{A}_2, \cdots, \mathbf{A}_Q] \in \mathcal{R}(\mathbf{A}) = \mathcal{R}(\mathbf{A}_q) \cup \mathcal{R}(\mathbf{A}_{q-}). \tag{14}$$

Similar to Eqn. (8), to the subspaces $\mathcal{R}(\mathbf{A}_q)$ and $\mathcal{R}(\mathbf{A}_{q-})$, the corresponding oblique projection matrices $\mathbf{E}_{q|q-}$ and $\mathbf{E}_{q-|q}$ are formulated as

$$\mathbf{E}_{q|q-} = \mathbf{A}_q(\mathbf{A}_q^H \mathbf{P}_{q-}^{\perp} \mathbf{A}_q)^{-1} \mathbf{A}_q^H \mathbf{P}_{q-}^{\perp}, \tag{15}$$

$$\mathbf{E}_{q-|q} = \mathbf{A}_{q-}(\mathbf{A}_{q-}^H \mathbf{P}_{q}^{\perp} \mathbf{A}_{q-})^{-1} \mathbf{A}_{q-}^H \mathbf{P}_{q}^{\perp}. \tag{16}$$

As presented in Eqn. (9), the orthogonal projection matrix $\mathbf{P}_A = \mathbf{A}(\mathbf{A}^H\mathbf{A})^{-1}\mathbf{A}^H$ to the L dimensional subspace $\mathcal{R}(\mathbf{A})$ can be expressed as the sum of two oblique projection matrices, that is, $\mathbf{P}_A = \mathbf{E}_{q|q-} + \mathbf{E}_{q-|q}$. Also, $\mathbf{P}_A$ can be formulated as the sum of Q oblique projection matrices as

$$\mathbf{P}_A = \mathbf{E}_{q|q-} + \mathbf{E}_{q-|q} = \sum_{q=1}^{Q} \mathbf{E}_{q|q-}. \tag{17}$$

The Eqn. (17) indicates that the orthogonal projection vector $\mathbf{p}$ can be decomposed into the sum of Q vectors as

$$\mathbf{p} = \mathbf{P}_A \mathbf{b} = \sum_{q=1}^{Q} \mathbf{p}_q, \tag{18}$$

where $\mathbf{p}_q = \mathbf{E}_{q|q-}\mathbf{b}$ is the oblique projection vector of the vector $\mathbf{b}$ onto the subspace $\mathcal{R}(\mathbf{A}_q)$.

Moreover, the computational properties in Eqn. (10) can be extended to the scenario with Q subspaces, for $q = 1, 2, \cdots, Q$, which are formulated as

$$\mathbf{E}_{q|q-}\mathbf{A}_i = \begin{cases} \mathbf{A}_i, & i = q, \\ \mathbf{0}, & i \neq q, \end{cases} \tag{19}$$

$$\mathbf{E}_{q-|q}\mathbf{A}_i = \begin{cases} \mathbf{0}, & i = q, \\ \mathbf{A}_i, & i \neq q. \end{cases} \tag{20}$$

V. Oblique Projection based Secret Communication

In this section, we present the oblique projection based secret communication scheme which consists of the following four phases: Low Sidelobe Transmitting Pattern Optimization, Oblique Projection Matrix Construction, Multiuser Constellation Syntheses and AN Generation. The first and the second phases are only executed if the channel changes. The third and fourth phases are executed in each symbol period until the channel changes. In the first phase, with the known knowledge about target users' channels, a primary transmitting weight vector is obtained by optimization algorithms under the constraint of multiple-beam pattern along with low sidelobes. In the second phase, a transformation matrix constituted with the aid of oblique projection matrix is also obtained from the channel knowledge. In the third phase, the symbols of interest are synthesized to the corresponding target users at symbol rate, with the obtained primary transmitting weight vector and the transformation matrix. In the fourth phase, the AN is superimposed to the undesired directions.

A. Low Sidelobe Transmitting Pattern Optimization

Given the channel vector of the k-th target user $\mathbf{h}_k = \mathbf{a}(\theta_k)$, for $k = 1, 2, \cdots, K$, the transmitting pattern of the BS is designed to have K beams along with low sidelobes. Thus, the transmitting power of the antenna can be focused on the target directions to improve the received SNR of the target users. Meanwhile, it increases the difficulties for the eavesdroppers to obtain the information of the target receivers, since the power leaked to the undesired directions is low. Similar to Eqn. (5), the design of low sidelobe pattern with multi-beams can be expressed as the following constrained optimization problem:

$$\begin{aligned} &\min_{\mathbf{w}} (\rho); \\ &\text{subject to } \mathbf{w}^H\mathbf{a}(\theta_k) = 1, k = 1, 2, \cdots, K; \\ &\left|\mathbf{w}^H\mathbf{a}(\theta)\right| \leq \rho, \theta \in \Theta, \end{aligned} \tag{21}$$

where K mainlobes are defined by constraint $\mathbf{w}^H\mathbf{a}(\theta_k) = 1$, and the low sidelobes are obtained by minimizing the pattern level within the angular range Θ.

The Prob. (21) is a typical constrained optimization problem, many existing algorithms [35]–[37] can be adopted to solve it. With the obtained numerical result $\mathbf{w}_L$, the transmitting pattern $\left|\mathbf{w}_L^H\mathbf{a}(\theta)\right|$ with multiple beams and low sidelobes can be obtained. Note that the details of the optimization solutions are not discussed in this paper.

B. Oblique Projection Matrix Construction

Given the K single-path target users with channel vectors $\mathbf{h}_k = \mathbf{a}(\theta_k)$, for $k = 1, 2, \cdots, K$, an additional steering vector $\mathbf{a}(\theta_0) \neq \mathbf{a}(\theta_k)$, is introduced to produce AN. With these $K+1$ vectors, the matrix $\mathbf{A}$ can be constructed as

$$\mathbf{A} = [\mathbf{a}(\theta_0), \mathbf{a}(\theta_1), \cdots, \mathbf{a}(\theta_K)] \in C^{N\times(K+1)}. \tag{22}$$

According to Eqn. (14), the matrix $\mathbf{A}$ can be partitioned as

$$\mathbf{A} = [\mathbf{a}(\theta_0), \mathbf{a}(\theta_1), \cdots, \mathbf{a}(\theta_K)] \in \mathcal{R}(\mathbf{A}_k) \cup \mathcal{R}(\mathbf{A}_{k-}), \tag{23}$$

where $\mathbf{A}_k = \mathbf{a}(\theta_k)$, and the matrix $\mathbf{A}_{k-}$ is constituted by removing the column k from the matrix $\mathbf{A}$, i.e.,

$$\mathbf{A}_{k-} = [\mathbf{a}(\theta_0), \cdots, \mathbf{a}(\theta_{k-1}), \mathbf{a}(\theta_{k+1}), \cdots, \mathbf{a}(\theta_K)] \in C^{N\times K}. \tag{24}$$

According to Eqn. (15) and Eqn. (16), the oblique projection matrices $\mathbf{E}_{k|k-}$ and $\mathbf{E}_{k-|k}$ to subspaces $\mathcal{R}(\mathbf{A}_k)$ and $\mathcal{R}(\mathbf{A}_{k-})$ can be described as

$$\mathbf{E}_{k|k-} = \mathbf{A}_k(\mathbf{A}_k^H \mathbf{P}_{k-}^{\perp} \mathbf{A}_k)^{-1} \mathbf{A}_k^H \mathbf{P}_{k-}^{\perp} \in C^{N\times N}, \tag{25}$$

$$\mathbf{E}_{k-|k} = \mathbf{A}_{k-}(\mathbf{A}_{k-}^H \mathbf{P}_{k}^{\perp} \mathbf{A}_{k-})^{-1} \mathbf{A}_{k-}^H \mathbf{P}_{k}^{\perp} \in C^{N\times N}, \tag{26}$$

where $\mathbf{P}_k^{\perp}$ and $\mathbf{P}_{k-}^{\perp}$ are the orthogonal projection matrices to the orthogonal complement space of the subspaces $\mathcal{R}(\mathbf{A}_k)$ and $\mathcal{R}(\mathbf{A}_{k-})$, respectively. $\mathbf{P}_k^{\perp}$ and $\mathbf{P}_{k-}^{\perp}$ are

$$\mathbf{P}_k^{\perp} = \mathbf{I} - \mathbf{A}_k(\mathbf{A}_k^H\mathbf{A}_k)^{-1}\mathbf{A}_k^H \in C^{N\times N}, \tag{27}$$

$$\mathbf{P}_{k-}^{\perp} = \mathbf{I} - \mathbf{A}_{k-}(\mathbf{A}_{k-}^H\mathbf{A}_{k-})^{-1}\mathbf{A}_{k-}^H \in C^{N\times N}. \tag{28}$$

C. Multiuser Constellation Syntheses

Now we have the primary transmitting weight vector $\mathbf{w}_L$ and the oblique projection matrices $\mathbf{E}_{k|k-}$ and $\mathbf{E}_{k-|k}$, where $k = 1, 2, \cdots, K$. Note that $\mathbf{w}_L$, $\mathbf{E}_{k|k-}$, and $\mathbf{E}_{k-|k}$ all depend on the target users' steering vectors $\mathbf{a}(\theta_k)$, $k = 1, 2, \cdots, K$, respectively. That is, they only need to be renewed when the target user channels are changed.

Here, we present the details of constellation synthesis for the target users at each symbol period. With $\mathbf{w}_L$, $\mathbf{E}_{k|k-}$, and $\mathbf{E}_{k-|k}$, for $k = 1, 2, \cdots, K$, we define a transformation matrix $\mathbf{T}$ as

$$\mathbf{T} = \left(\mathbf{I} - \mathbf{E}_{0-|0}^H\right) + \sum_{k=1}^{K} c_k\mathbf{E}_{k|k-}^H \in C^{N\times N}, \tag{29}$$

where the oblique projection matrices are defined in Eqn. (25) and Eqn. (26), and c_k is a complex value to be determined.

With the primary transmitting weight vector $\mathbf{w}_L$, we define a disturbed weight vector $\mathbf{w}_0$ as

$$\mathbf{w}_0 = \mathbf{w}_L\left(\delta e^{j\psi}\right), \tag{30}$$

where the random complex $\delta e^{j\psi}$ can be assigned at each symbol period to produce AN.

Then, the transmitting weight vector $\mathbf{w}_s$ of the BS is defined as the linear transformation on $\mathbf{w}_0$ based on the transformation matrix $\mathbf{T}$, which is given as

$$\mathbf{w}_s = \mathbf{T}\mathbf{w}_0 = \left[\left(\mathbf{I} - \mathbf{E}_{0-|0}^H\right) + \sum_{k=1}^{K} c_k\mathbf{E}_{k|k-}^H\right]\mathbf{w}_0. \tag{31}$$

Thus, the antenna response to the k^{th} target user at the direction θ_k can be described as

$$\mathbf{w}_s^H\mathbf{a}(\theta_k) = \mathbf{w}_0^H\left[\left(\mathbf{I} - \mathbf{E}_{0-|0}\right) + \sum_{n=1}^{K} c_n^*\mathbf{E}_{n|n-}\right]\mathbf{a}(\theta_k). \tag{32}$$

With the properties of the oblique projection matrices described in Eqn. (19) and Eqn. (20), we have

$$\begin{aligned}&\mathbf{E}_{0-|0}\mathbf{a}(\theta_k) = \mathbf{a}(\theta_k),\\ &\left[\sum_{n=1}^{K} c_n^*\mathbf{E}_{n|n-}\right]\mathbf{a}(\theta_k) = \mathbf{a}(\theta_k).\end{aligned} \tag{33}$$

Thus, the antenna response in Eqn. (32) can be simplified as

$$\mathbf{w}_s^H\mathbf{a}(\theta_k) = c_k^*\mathbf{w}_0^H\mathbf{a}(\theta_k), \tag{34}$$

so the antenna response at the direction θ_k depends on c_k, rather than c_n, for $n = 1, 2, \cdots, K$, $n \neq k$.

Given $\mathbf{w}_0$ and $\mathbf{a}(\theta_k)$, their inner product $\mathbf{w}_0^H\mathbf{a}(\theta_k)$, which is a complex number, can be represented with the amplitude B_k and the phase φ_k as

$$\mathbf{w}_0^H\mathbf{a}(\theta_k) = \left|\mathbf{w}_0^H\mathbf{a}(\theta_k)\right| e^{j\varphi_k} = B_k e^{j\varphi_k}. \tag{35}$$

If a desired symbol $e^{j\alpha_k}$ along with the gain γ_k of the k^{th} target user is $\gamma_k s_k = \gamma_k e^{j\alpha_k}$, that is, $\mathbf{w}_s^H\mathbf{a}(\theta_k) = \gamma_k e^{j\alpha_k}$ is expected by the k^{th} target user, then, the complex parameter c_k can be solved via Eqn. (34) and Eqn. (35) as

$$c_k = (\gamma_k/B_k)\, e^{j\varphi_k - j\alpha_k}. \tag{36}$$

By substituting c_k in Eqn. (34), the antenna response at the k^{th} target user's direction θ_k is the same as the desired value, which is

$$\mathbf{w}_s^H\mathbf{a}(\theta_k) = c_k^*\mathbf{w}_0^H\mathbf{a}(\theta_k) = \gamma_k e^{j\alpha_k}. \tag{37}$$

Thus, the expected symbol $e^{j\alpha_k}$ and the gain γ_k for the k^{th} target user can be synthesized correctly, given c_k in Eqn. (36) and $\mathbf{w}_s$ in Eqn. (31). By substituting c_k in Eqn. (36), for $k = 1, 2, \cdots, K$, in Eqn. (31), respectively, we have $\mathbf{w}_s$ that enables multicast communication, where each desired symbol $\gamma_k e^{j\alpha_k}$ can be synthesized at the direction θ_k for the k^{th} target user simultaneously. Therefore, the multicast communication with K target users is achieved.

D. AN Generation

In this section, we present the AN generation based on oblique projection, which is used for adding randomness to the received signal at the undesired directions.

With the primary transmitting weight vector $\mathbf{w}_L$, the antenna response at the direction θ_0 is

$$\mathbf{w}_L^H\mathbf{a}(\theta_0) = \left|\mathbf{w}_L^H\mathbf{a}(\theta_0)\right| e^{j\varphi_0} = B_0 e^{j\varphi_0}, \tag{38}$$

where B_0 and φ_0 can be taken as the initial magnitude and phase of the response, respectively. Furthermore, the antenna response at the direction θ_0 with the disturbed weight vector $\mathbf{w}_0$ in Eqn. (30) is given by

$$\mathbf{w}_0^H\mathbf{a}(\theta_0) = \left|\mathbf{w}_0^H\mathbf{a}(\theta_0)\right| e^{j\psi + j\varphi_0} = (B_0\delta)\, e^{j\psi + j\varphi_0}. \tag{39}$$

According to the oblique projection matrix in Eqn. (33), we have

$$\begin{aligned}&\mathbf{E}_{0-|0}\mathbf{a}(\theta_0) = 0,\\ &\left[\sum_{k=1}^{K} c_k^*\mathbf{E}_{k|k-}\right]\mathbf{a}(\theta_0) = 0.\end{aligned} \tag{40}$$

By substituting the above results in the antenna response $\mathbf{w}_s^H\mathbf{a}(\theta_0)$ at the direction θ_0 with the weight vector $\mathbf{w}_s$ in Eqn. (31), $\mathbf{w}_s^H\mathbf{a}(\theta_0)$ can be simplified as

$$\mathbf{w}_s^H\mathbf{a}(\theta_0) = \mathbf{w}_0^H\mathbf{a}(\theta_0) = (B_0\delta)\, e^{j\psi + j\varphi_0}. \tag{41}$$

Following Eqn. (41), the disturbing complex number $\delta e^{j\psi}$ in Eqn. (30) is eventually obtained in the antenna response at the direction θ_0 through the transmitting weight vector $\mathbf{w}_s$. Note that this disturbing complex number does not affect the antenna response at the desired direction θ_k, for $k = 1, 2, \cdots, K$, as shown in Eqn. (37), since it is offset by c_k in Eqn. (36). In other words, the symbol transmissions from the BS to the target users are independent to the disturbing complex number $\delta e^{j\psi}$.

Algorithm 1 Computing Steps of Transmitting Weight Vector

Input: The target user steering vectors $\mathbf{a}(\theta_k)$, $k = 1, 2, \cdots, K$, respectively.
Initialize: Solve optimization in Eqn. (21) find the primary weight vector $\mathbf{w}_L$.
for $k = 1, 2, \cdots,$ K **do**
  $\mathbf{A}_k = \mathbf{a}(\theta_k)$.
  $\mathbf{A}_{k-} = [\mathbf{a}(\theta_0), \cdots, \mathbf{a}(\theta_{k-1}), \mathbf{a}(\theta_{k+1}), \cdots, \mathbf{a}(\theta_K)]$.
  $\mathbf{P}_k^{\perp} = \mathbf{I} - \mathbf{A}_k(\mathbf{A}_k^H\mathbf{A}_k)^{-1}\mathbf{A}_k^H$.
  $\mathbf{P}_{k-}^{\perp} = \mathbf{I} - \mathbf{A}_{k-}(\mathbf{A}_{k-}^H\mathbf{A}_{k-})^{-1}\mathbf{A}_{k-}^H$.
  $\mathbf{E}_{k|k-} = \mathbf{A}_k(\mathbf{A}_k^H\mathbf{P}_{k-}^{\perp}\mathbf{A}_k)^{-1}\mathbf{A}_k^H\mathbf{P}_{k-}^{\perp}$.
  $\mathbf{E}_{k-|k} = \mathbf{A}_{k-}(\mathbf{A}_{k-}^H\mathbf{P}_k^{\perp}\mathbf{A}_{k-})^{-1}\mathbf{A}_{k-}^H\mathbf{P}_k^{\perp}$.
end for
for Each symbol period **do**
  $\mathbf{w}_0 = \mathbf{w}_L\left(\delta e^{j\psi}\right)$ with random number $\delta e^{j\psi}$.
  for Each symbol $\gamma_k e^{j\alpha_k}$, $k = 1, 2, \cdots,$ K **do**
    $B_k e^{j\varphi_k} = \mathbf{w}_0^H\mathbf{a}(\theta_k)$.
    $c_k = (\gamma_k/B_k)\, e^{j\varphi_k - j\alpha_k}$.
  end for
  $\mathbf{T} = \left(\mathbf{I} - \mathbf{E}_{0-|0}^H\right) + \sum_{k=1}^{K} c_k\mathbf{E}_{k|k-}^H$.
  Output: Transmitting weight vector $\mathbf{w}_s = \mathbf{T}\mathbf{w}_0$.
end for
if Channel is changed **then**
  Go to step 2.
else
  Go to step 11.
end if

In contrast, the antenna response to other undesired direction θ ($\theta \neq \theta_k$) with the weight vector $\mathbf{w}_s$ in Eqn. (31) is

$$\mathbf{w}_s^H\mathbf{a}(\theta) = \left(\delta e^{j\psi}\right)^*\mathbf{w}_L^H\left[\left(\mathbf{I} - \mathbf{E}_{0-|0}\right) + \sum_{k=1}^{K} c_k^*\mathbf{E}_{k|k-}\right]\mathbf{a}(\theta). \tag{42}$$

It can be found that the disturbing complex number $\delta e^{j\psi}$ is merged with the antenna response at other undesired directions.

By randomly changing the disturbing complex number $\delta e^{j\psi}$ in Eqn. (30) at symbol rate, the random amplitude and phase are superposed to the received signals of all eavesdroppers. Thus, the received constellations are scrambled and cannot be demodulated by the eavesdroppers correctively. To keep the transmitting pattern with low sidelobes, it is suggested that the amplitude disturbing δ takes the value close to 1. If $\delta = 1$, the communication secrecy can still be achieved with only the random phase applied on the received signals of eavesdroppers.

In summary, the transmitting weight vector update algorithm for secret communication based on the oblique projection is described in Algorithm 1.

VI. Performance Evaluation and Discussion

In this section, we conduct the analysis on communication secrecy, computational complexity, and low sidelobe characteristic of the proposed scheme.

A. Communication Secrecy

Exploiting Algorithm 1, we obtain a secret multicast mmWave transmission scheme with low sidelobe transmitting pattern based on the linear transformation on the optimized low sidelobe primary weight vector with the aid of the oblique projection operator. The pattern mainlobes are devised toward target users' directions to guarantee the effective transmission of the intended symbols. The low sidelobe transmitting pattern can achieve low SNRs of the eavesdroppers' received signals at the undesired directions. It provides a certain level of protection on the communication secrecy with the increased difficulties for the eavesdroppers in demodulating constellations due to the low received SNRs.

By setting the parameter c_k in the transformation matrix $\mathbf{T}$ in Eqn. (36) at each time instant of a symbol, the symbol $e^{j\alpha_k}$ together with gain γ_k in Eqn. (37) can be synthesized to the corresponding direction of the k^{th} target user. That is, the antenna response at the direction θ_k exactly equals to $\gamma_k e^{j\alpha_k}$. With the same transmitting weight vector $\mathbf{w}_s$ in Eqn. (31), the antenna response $\mathbf{w}_s^H\mathbf{a}(\theta)$ at other undesired direction θ, $\theta \neq \theta_k$, can be described as

$$\mathbf{w}_s^H\mathbf{a}(\theta) = \mathbf{w}_0^H\left[\left(\mathbf{I} - \mathbf{E}_{0-|0}\right) + \sum_{k=1}^{K} c_k^*\mathbf{E}_{k|k-}\right]\mathbf{a}(\theta), \tag{43}$$

which indicates that the antenna response at other undesired direction θ is affected by all K parameters $c_k, k = 1, 2, \cdots, K$, respectively. Thus, each symbol can be hardly separated from the received signals at undesired directions.

If there are L constellation states for the symbol $s_k = e^{j\alpha_k}$ with a certain modulation, then c_k takes one of the L possible values in Eqn. (36) at each time instant. Considering that there are K users in the system, the weight vector $\mathbf{w}_s$ in Eqn. (31) can be in one of the L^K different statuses. For example, with a QPSK modulation system with 4 target users, the possible number of the weight vector $\mathbf{w}_s$ statuses is $L^K = 256$. Usually, at each different time instant, a different weight vector in one of the L^K statuses is generated as the transmitting weight vector for the PLS communication system. Therefore, the received symbols towards the undesired eavesdroppers are scrambled, since the transmitting weight vector varies at symbol rate.

More importantly, the AN technique based on oblique projection is adopted. At each time instant, by randomly varying the complex number $\delta e^{j\psi}$ in Eqn. (30), the received signals by the eavesdroppers are scrambled by the random amplitude and phase. Thus, the transmitted constellations can hardly be accurately extracted by the eavesdroppers.

B. Computational Complexity

In this section, we discuss the computational complexity of the proposed secret communication scheme.

The computation of the transmitting weight vector $\mathbf{w}_s$ in Eqn. (31) has two stages. The first stage takes place at each channel update cycle, and the second occurs at every symbol period.

For the first stage at each channel update cycle, with the knowledge of the K target users' steering vectors $\mathbf{a}(\theta_k)$, for

$k = 1, 2, \cdots, K$, the primary transmitting weight vector $\mathbf{w}_L$ can be obtained by adopting some widely used optimization approaches, such as convex optimization with the computational complexity of $\mathcal{O}[N^{3.5}\log(1/\epsilon)]$ [33], where N is the number of array elements and ϵ is the solution accuracy. In this stage, the oblique projection matrices $\mathbf{E}_{k|k-}$ and $\mathbf{E}_{k-|k}$, for $k = 1, 2, \cdots, K$, are computed in Eqn. (25) and Eqn. (26). Note that most of the computational complexities come from the matrix inversion in Eqn. (26) and Eqn. (28). The computational complexity is $\mathcal{O}(K^3)$ for the k^{th} user, here K is the number of target users. Thus, for $k = 1, 2, \cdots, K$, the overall computational complexity for the first stage is estimated as $\mathcal{O}(K^4)$. It should be pointed out that the computational burden in the first stage is affordable for the computational hardware resources on the BS. This is because the computation of the primary weight vector $\mathbf{w}_L$, the oblique projection matrices $\mathbf{E}_{k|k-}$ and $\mathbf{E}_{k-|k}$, for $k = 1, 2, \cdots, K$, are performed only once in each channel update period. Usually, the channel update period is relatively long.

For the second stage, at each time instant for symbol transmission, the transmitting weight vector update computations cover the Step 12 to the Step 18 in Algorithm 1. The computations of Step 14 and Step 15 only involve the multiplications of numbers and inner product of two vectors. In Step 17, a linear transformation of the weight vector is computed. Thus, the computational complexity in the second stage at each symbol instant is acceptable.

Therefore, the overall computational complexity is low for the hardware on the BS.

C. Low Sidelobe Analysis of Weight Vector $\mathbf{w}_s$

The transmitting weight vector $\mathbf{w}_s$ in the proposed scheme is the result of linear transformation on the weight vector $\mathbf{w}_0$ in Eqn. (31). The primary weight vector $\mathbf{w}_L$ obtained from the optimization problem in Eqn. (21) has the low sidelobe characteristic. Because the weight vector $\mathbf{w}_0$ is the product of $\mathbf{w}_L$ and the scalar $\delta e^{j\psi}$, $\left|\mathbf{w}_0^H \mathbf{a}(\theta)\right|$ maintains the low sidelobe transmitting pattern. Here, we discuss the low sidelobe characteristic of the transmitting weight vector $\mathbf{w}_s$.

The Eqn. (31) can be rewritten as

$$\mathbf{w}_s = \mathbf{w}_0 - \mathbf{E}_{0-|0}^H \mathbf{w}_0 + \left[\sum_{k=1}^{K} c_k \mathbf{E}_{k|k-}^H\right] \mathbf{w}_0. \tag{44}$$

By setting $\mathbf{P}_A = \mathbf{E}_{0-|0} + \mathbf{E}_{0|0-}$, we have

$$\mathbf{w}_s = \mathbf{w}_0 - \mathbf{P}_A \mathbf{w}_0 + \mathbf{E}_{0|0-}^H \mathbf{w}_0 + \left[\sum_{k=1}^{K} c_k \mathbf{E}_{k|k-}^H\right] \mathbf{w}_0. \tag{45}$$

According to Eqn. (47) in [29], we have the oblique projection of the vector $\mathbf{w}_0$ as

$$\mathbf{E}_{k|k-}^H \mathbf{w}_0 = \xi_k \mathbf{a}^H(\theta_k)\, \mathbf{w}_0 \mathbf{A} \mathbf{g}_k, k = 0, 1, 2, \cdots K, \tag{46}$$

where

$$\xi_k = \left[\mathbf{a}^H(\theta_k)\, \mathbf{P}_{k-}^{\perp} \mathbf{a}(\theta_k)\right]^{-1}, \tag{47}$$

$$\mathbf{g}_k = \left[g_1^{(k)}, \cdots, g_k^{(k)}, 1, g_{k+1}^{(k)}, \cdots, , g_{K-1}^{(k)}\right]^T, \tag{48}$$

$g_i^{(k)}$ is the i^{th} element of the vector $-\left[\mathbf{A}_{k-}^H \mathbf{A}_{k-}\right]^{-1} \mathbf{A}_{k-}^H \mathbf{a}(\theta_k)$.

Since $\mathbf{a}^H(\theta_k)\, \mathbf{w}_0$ is a scalar, Eqn. (46) is further altered as

$$\mathbf{E}_{k|k-}^H \mathbf{w}_0 = \mathbf{A} \xi_k \mathbf{a}^H(\theta_k)\, \mathbf{w}_0 \mathbf{g}_k, k = 0, 1, 2, \cdots K. \tag{49}$$

By substituting the orthogonal projection matrix $\mathbf{P}_A = \mathbf{A}(\mathbf{A}^H\mathbf{A})^{-1}\mathbf{A}^H$ and Eqn. (49) into Eqn. (45), we simply Eqn. (45) as

$$\mathbf{w}_s = \mathbf{w}_0 + \mathbf{A}\mathbf{f}, \tag{50}$$

where the column $\mathbf{f} = [f_0, f_1, \cdots, f_K]^T \in C^{(K+1)\times 1}$ can be formulated as

$$\mathbf{f} = -(\mathbf{A}^H\mathbf{A})^{-1}\mathbf{A}^H\mathbf{w}_0 + \xi_0 \mathbf{a}^H(\theta_0)\, \mathbf{w}_0 \mathbf{h}_0 + \left[\sum_{k=1}^{K} c_k \xi_k \mathbf{a}^H(\theta_k)\, \mathbf{w}_0 \mathbf{h}_k\right]. \tag{51}$$

Eqn. (50) indicates that the transmitting weight vector $\mathbf{w}_s$ is the sum of the weight vector $\mathbf{w}_0$ in a low sidelobe level and a correction vector $\mathbf{A}\mathbf{f}$. Considering that $\mathbf{A} = [\mathbf{a}(\theta_0), \mathbf{a}(\theta_1), \cdots, \mathbf{a}(\theta_K)]$, $\mathbf{A}\mathbf{f}$ is the linear combination of the target users' steering vectors $\mathbf{a}(\theta_k)$, for $k = 0, 1, \cdots, K$. Thus, we have

$$\mathbf{w}_s = \mathbf{w}_0 + \sum_{k=0}^{K} [f_k \mathbf{a}(\theta_k)]. \tag{52}$$

With the weight vector $\mathbf{w}_s$, the antenna response to the undesired direction θ ($\theta \neq \theta_k$, $k = 0, 1, \cdots, K$) is

$$\mathbf{w}_s^H \mathbf{a}(\theta) = \mathbf{w}_0^H \mathbf{a}(\theta) + \sum_{k=0}^{K} \left[f_k \mathbf{a}^H(\theta_k)\, \mathbf{a}(\theta)\right]. \tag{53}$$

Here, the first term on the right side is the antenna response with the weight vector $\mathbf{w}_0$, which has a low sidelobe level. The second term is the sum of $K+1$ inner products $\mathbf{a}^H(\theta_k)\, \mathbf{a}(\theta)$, for $k = 0, 1, \cdots, K$, respectively. Each inner product can be taken as the antenna pattern with the weight vector $\mathbf{a}(\theta_k)$. We know that the first sidelobe level of the pattern $\mathbf{a}^H(\theta_k)\, \mathbf{a}(\theta)$ is 13.4 dB lower than its mainlobe. Thus, within the sidelobe ranges of the angles, the second term on the right side of Eqn. (53) has lower levels. As a result, the transmitting weight vector $\mathbf{w}_s$ for the secret multicast communication still has the low sidelobe characteristic, which indicates that the transformation matrix $\mathbf{T}$ does not significantly change the antenna pattern sidelobe levels of the primary weight vector $\mathbf{w}_0$.

In addition, the vector $\mathbf{A}\mathbf{f}$ is the linear combination of all target users' steering vectors belonging to the subspace $\mathcal{R}(\mathbf{A})$. However, the vector $\mathbf{a}(\theta)$ deviates from the steering vectors and belongs to the orthogonal complement space of $\mathcal{R}(\mathbf{A})$, i.e., $\mathbf{a}(\theta) \in \mathcal{R}^{\perp}(\mathbf{A})$. Thus, the inner product $\mathbf{a}^H(\theta_k)\, \mathbf{a}(\theta)$ is much smaller than that of the target direction $\theta = \theta_k$, for $k = 0, 1, \cdots, K$. The antenna pattern $\mathbf{w}_s^H \mathbf{a}(\theta)$ can keep the approximately same low sidelobe characteristic as that of the antenna pattern $\mathbf{w}_0^H \mathbf{a}(\theta)$.

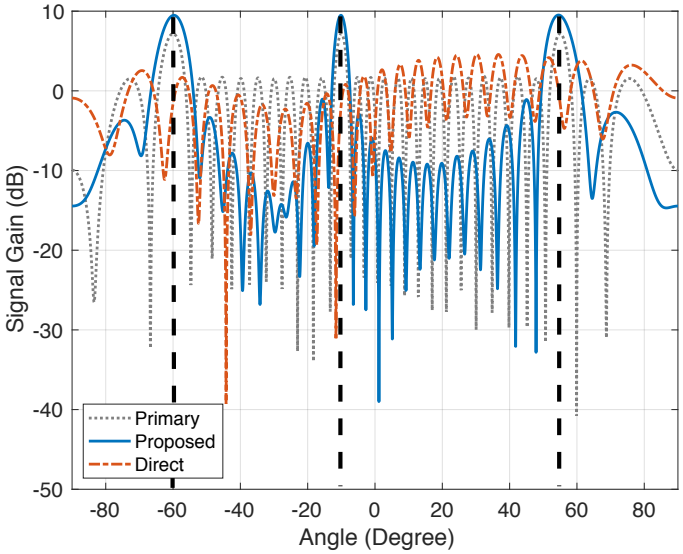

Fig. 3. The low sidelobe transmitting pattern with 3 target users located at the angles of $-60°$, $-10°$ and $55°$.

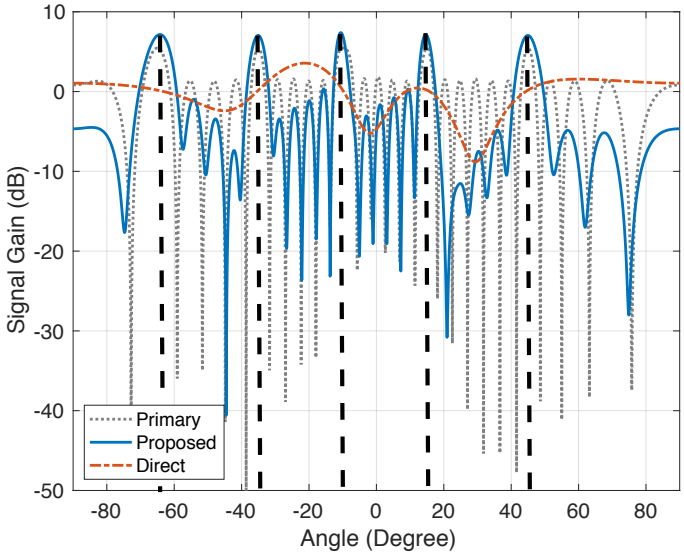

Fig. 4. The low sidelobe transmitting pattern with 5 target users located at the angles of $-65°$, $-35°$, $-10°$, $15°$ and $45°$.

VII. Simulation Results

In this section, we conduct the simulations to validate the superiorities of the proposed scheme for mmWave communication. The system has a BS equipped with an ULA of $N = 30$, where the antenna space is $d = \lambda/2$. We assume the system is under single-path channels with Additive White Gaussian Noise (AWGN).

A. Multiuser Low Sidelobe Transmitting Pattern

We demonstrate the validity of the multiuser low sidelobe transmitting pattern designed in the Section V-A and analyzed in the Section VI-C, respectively.

Fig. 3 shows the low sidelobe transmitting pattern of three target users located at the angles of $-60°$, $-10°$ and $55°$, respectively. The gray dashed line is the transmitting pattern $\left|\mathbf{w}_L^H \mathbf{a}(\theta)\right|$ based on the primary transmitting weight vector $\mathbf{w}_L$, which is the result of the constrained optimization problem in Eqn. (21). The pattern mainlobe gains toward the target user directions are about 6.5 dB higher than that at sidelobe directions. With the higher received SNRs, the target users have better communication performance.

The blue solid line stands for the transmitting pattern $\left|\mathbf{w}_s^H \mathbf{a}(\theta)\right|$, which is based on the weight vector $\mathbf{w}_s$ obtained from Eqn. (31). From Fig. 3, the transmitting pattern of the proposed scheme has the low sidelobe characteristic. It demonstrates the validity of the analysis in the Section VI-C that the transformation matrix $\mathbf{T}$ does not significantly change the sidelobe levels of the transmitting pattern. In contrast, the transmitting pattern based on the weight vector $\mathbf{w}_D$ in the red dashed line, which is obtained from the solution of the equation set in Eqn. (4), does not have the low sidelobe pattern. The transmitting power is not concentrated on the target users' directions.

In Fig. 4, we present a low sidelobe transmitting pattern of five target users located at the angles of $-65°$, $-35°$, $-10°$, $15°$ and $45°$. The similar results above can be obtained. The sidelobe level is about 4.5 dB lower than that of the mainlobe. In general, the increasing number of the mainlobes of the transmitting pattern leads to higher levels of the sidelobes.

B. Multiuser Constellation Syntheses

To intuitively observe the performance of the proposed scheme, we conduct the constellation synthesis simulation for multiple target users. We consider different modulation types, such as QPSK and 16-Quadrature Amplitude Modulation (QAM). For simplicity, δ in Eqn. (30) is set to be $\delta = 1$.

1) QPSK: Suppose there are three target users (Bobs) located at the directions of $\theta_{B_1} = -60°$, $\theta_{B_2} = -10°$, and $\theta_{B_3} = 55°$, respectively. There are three eavesdroppers (Eves) with angular locations of $\theta_{E_1} = -16°$, $\theta_{E_2} = -1°$, and $\theta_{E_3} = 7°$. The angle θ_0 of the additional steering vector $\mathbf{a}(\theta_0)$ in Eqn. (22) for oblique projection matrix construction is set to be $\theta_0 = 80°$. The QPSK symbols are designed to transmit to the three target users. The random phase ψ is randomly selected in the range of $(0, 2\pi]$ at the symbol rate to generate AN. To highlight the performance of the proposed scheme, the received noise is ignored. The transmitting weight vector $\mathbf{w}_s$ is updated based on the steps in Algorithm 1. The noiseless antenna response at the direction θ_k can be obtained by $y_k = \mathbf{w}_s^H \mathbf{a}(\theta_k)$, for $k = 1, 2, 3$, respectively. In the complex plane, the drawings of the antenna responses y_k are the constellations. The simulation trial number is taken as 1000.

Fig. 5 shows the noiseless constellations of target users (Bobs) in blue and eavesdroppers (Eves) in red with QPSK. It is clear that Bobs' constellations are always in clear shapes. In contrast, Eves' noiseless constellations randomly scatter in the complex plane. Thus, only Bobs located at the target directions of $\theta_{B_1} = -60°$, $\theta_{B_2} = -10°$, and $\theta_{B_3} = 55°$ can correctly demodulate the received signal to obtain the

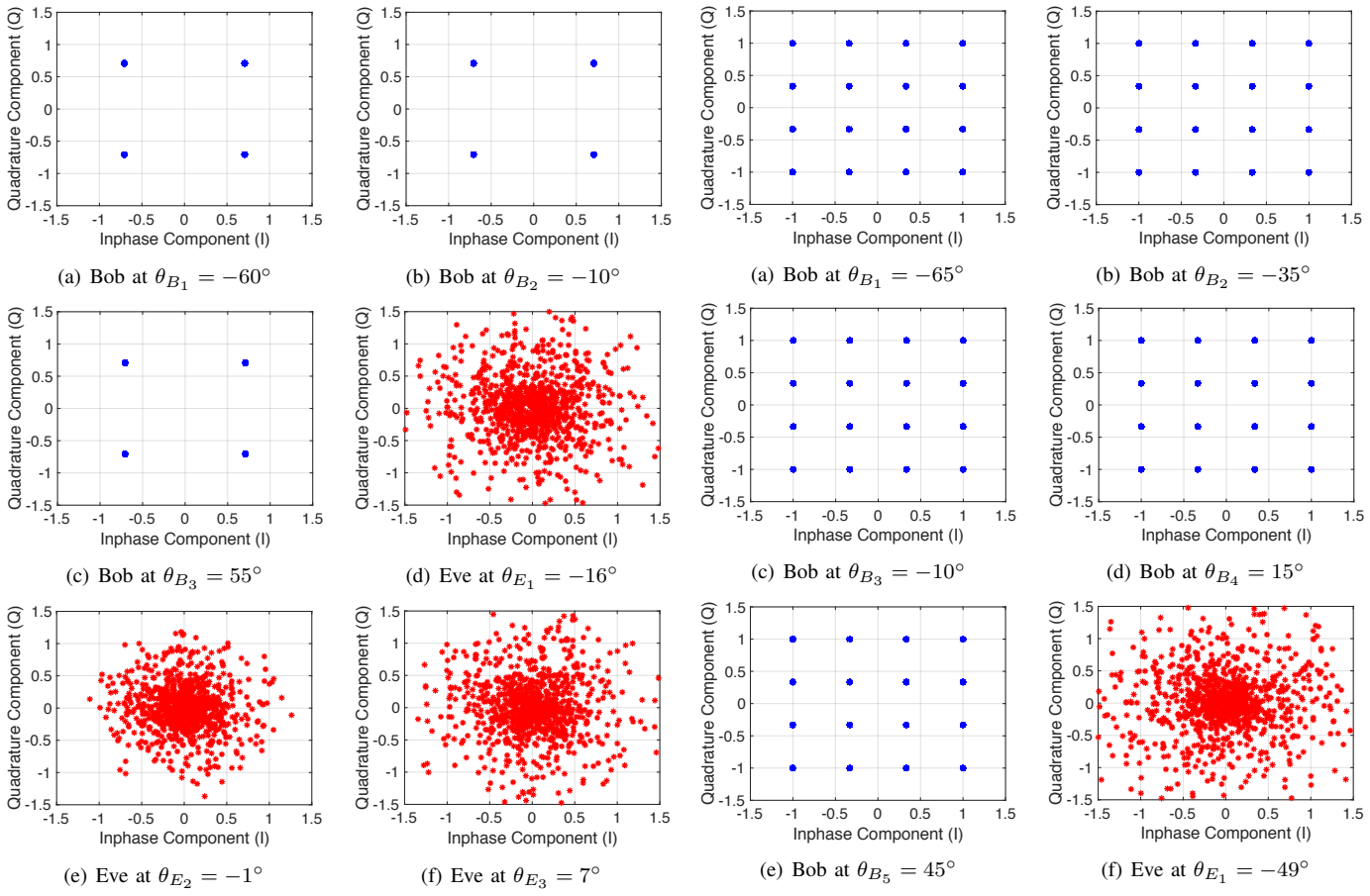

(a) Bob at $\theta_{B_1} = -60°$ (b) Bob at $\theta_{B_2} = -10°$ (c) Bob at $\theta_{B_3} = 55°$ (d) Eve at $\theta_{E_1} = -16°$ (e) Eve at $\theta_{E_2} = -1°$ (f) Eve at $\theta_{E_3} = 7°$

Fig. 5. Noiseless received constellations at Bobs and Eves using the proposed secret multicast transmission scheme with QPSK

(a) Bob at $\theta_{B_1} = -65°$ (b) Bob at $\theta_{B_2} = -35°$ (c) Bob at $\theta_{B_3} = -10°$ (d) Bob at $\theta_{B_4} = 15°$ (e) Bob at $\theta_{B_5} = 45°$ (f) Eve at $\theta_{E_1} = -49°$ (g) Eve at $\theta_{E_2} = 0°$ (h) Eve at $\theta_{E_3} = 29°$

Fig. 6. Noiseless received constellations at Bobs and Eves using the proposed secret multicast transmission scheme with 16-QAM

information. Eves at other directions, such as $\theta_{E_1} = -16°$, $\theta_{E_2} = -1°$, and $\theta_{E_3} = 7°$, can hardly demodulate the signals with the scrambled constellations.

2) 16-QAM: we conduct the simulation with the same system parameters for 16-QAM. Different from the user settings in QPSK, five Bobs located at the directions of $\theta_{B_1} = -65°$, $\theta_{B_2} = -35°$, $\theta_{B_3} = -10°$, $\theta_{B_4} = 15°$, and $\theta_{B_5} = 45°$ are considered. Besides, suppose there are three Eves located at the angles of $\theta_{E_1} = -49°$, $\theta_{E_2} = 0°$, and $\theta_{E_3} = 29°$.

Fig. 6 shows that with 16-QAM, similar scrambled noiseless constellations are received by Eves at the non-desired directions, while the constellations at Bobs are all in clear shapes.

C. Security Metrics

We demonstrate the security performance of the proposed scheme by observing the simulation results of Symbol Error Rate (SER).

1) SER versus SNR: The settings for Bobs and Eves are the same as that in the QPSK scenario in Section VII-B. The QPSK symbols are transmitted to three target users. For comparison, we consider different PLS communication schemes, including the proposed scheme in Algorithm 1, the Conventional Phased-Array (CPA) transmission scheme, and the Artificial Noise Transmission (ANT) method [17]. Besides, we also consider the scheme (Non-low), in which the transmitting weight vector is obtained by Eqn. (30) and Eqn. (31) but the weight vector $\mathbf{w}_L$ is replaced by $\mathbf{w}_D$ obtained from Eqn. (4).

If the transmitting weight vector of the PLS communication scheme is $\mathbf{w}$, the antenna response at the direction θ_k is computed as

$$y_k = \mathbf{w}^H \mathbf{a}(\theta_k) + v_k, \tag{54}$$

where $v_k \sim \mathcal{CN}\left(0, \sigma^2\right)$ is AWGN, for $k = 1, 2, \cdots, K$, respectively. To observe the performance of each PLS scheme versus SNR, we vary the variance of the received noise v_k. With the antenna response y_k, we delete the constellation symbols. Then, we estimate the SER of the PLS communication scheme by the Monte Carlo method.

Suppose there are three target users. Fig. 7(a) shows the SER of the target user at $\theta_{B_1} = -10°$. The SER of CPA is the lowest one. The reason is that the antenna pattern mainlobe of

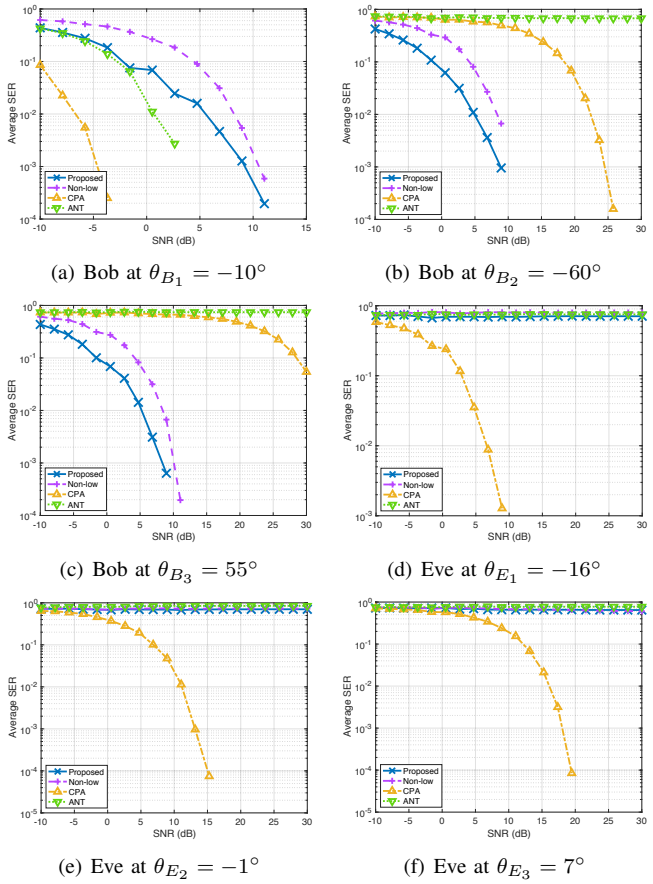

(a) Bob at $\theta_{B_1} = -10°$ (b) Bob at $\theta_{B_2} = -60°$

(c) Bob at $\theta_{B_3} = 55°$ (d) Eve at $\theta_{E_1} = -16°$

(e) Eve at $\theta_{E_2} = -1°$ (f) Eve at $\theta_{E_3} = 7°$

Fig. 7. Simulated SER versus SNR

CPA is designed to focus on this target user only. For the same reason, ANT also achieves low SER. In Fig. 7(a), the SER of the proposed scheme is lower than that of Non-low. This benefit comes from the low sidelobe antenna pattern design as presented in Fig. 3. Fig. 7(b) and Fig. 7(c) indicate the SERs of another two target users at $\theta_{B_2} = -60°$ and $\theta_{B_3} = 55°$, respectively. The SER of the proposed scheme is lower than that of Non-low. It is noticeable that the SERs of ANT in Fig. 7(b) and Fig. 7(c) are very high, it is because ANT only supports a single target user and two Bobs are not the target users for ANT. In addition, since the target users at $\theta_{B_1} = -60°$ and $\theta_{B_1} = 55°$ are located at the sidelobes of the CPA pattern, their SERs decrease with increase of SNR, but they are still much higher than that of the proposed scheme.

In Fig. 7(d), Fig. 7(e), and Fig. 7(f), we demonstrate the SER performance of three Eves at $\theta_{E_1} = -16°$, $\theta_{E_2} = -1°$, and $\theta_{E_3} = 7°$. The SERs of the proposed scheme, ANT and Non-low are all very high, even the SNR reaches up to 30 dB. It indicates that they all provide good protection on the communication secrecy. The SERs of CPA are low in Fig. 7(d), Fig. 7(e), and Fig. 7(f), since no PLS techniques are applied to them.

2) SER versus angle: To further observe the performance of the proposed scheme at all transmitting directions, we conduct a simulation on SER versus angle by varying the receiver direction from $-90°$ to $90°$. Suppose there are three Bobs at the directions of $-60°$, $-10°$, and $55°$, respectively. The

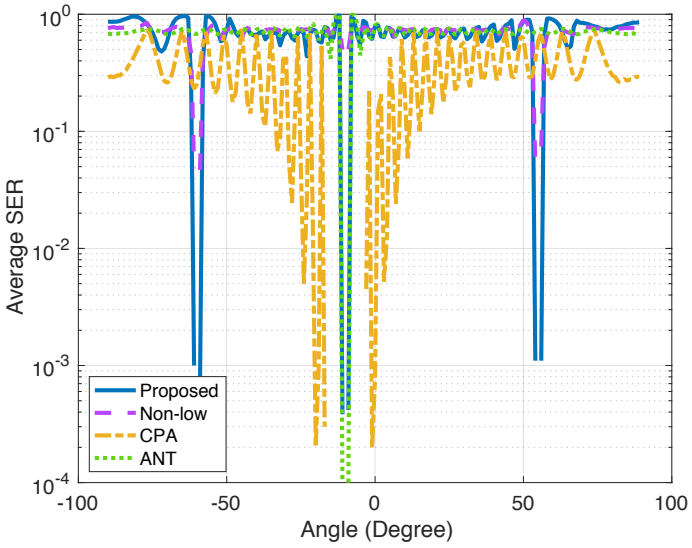

Fig. 8. SER versus angle of receiver (SNR=15dB)

QPSK is adopted. The SNR is set to be 15 dB.

The transmitting weight vector $\mathbf{w}_s$ can be obtained from Algorithm 1. As described in Eqn. (54), the antenna response at the direction θ can be computed as $y_\theta = \mathbf{w}^H \mathbf{a}(\theta) + v_\theta$. Then, the SERs can be estimated by the Monte Carlo method for the receiver at the direction θ. By varying the receiver direction θ from $-90°$ to $90°$, the SER versus angle curve can be obtained. Fig. 8 presents the simulation result of the proposed scheme in blue solid line. As expected, the SERs at the directions of the three Bobs are very low, which can guarantee the reliable communication of the target users. In contrast, the SERs at the undesired directions are extremely high, which demonstrates that the proposed scheme has good protection on the communication secrecy. As comparison, the SER curves in yellow and green belong to the CPA transmission scheme and the ANT scheme, respectively. CPA does not have any protection on the communication secrecy. Low SER can be obtained in many non-target directions. ANT can only achieve single user secret communication. Non-low has a similar SER curve to the proposed scheme, but its SERs at the target directions are slightly higher than that of the proposed scheme, since it does not have the low sidelobe pattern. This result is consistent to the simulation results in Fig. 7(b), Fig. 7(a), and Fig. 7(c).

VIII. Conclusions

In this paper, we have proposed the low sidelobe secret multicast transmission scheme by utilizing the PLS techniques to protect multicast mmWave communication. The low sidelobe transmitting pattern is exploited to enhance the communication performance for the target users, and the oblique projection approach is integrated to protect the optimized multicast communication without jeopardizing its low sidelobe transmitting pattern. With the transmission secrecy, the received data of the multiple target users at the desired directions are protected, and the eavesdroppers at the undesired directions cannot acquire any useful information. In addition, the proposed

scheme is affordable for the practical implementation due to its low computational complexity in weight vector update at each symbol period, such that it is particularly suitable for the scenarios where the communication entities do not have powerful computing capability, such as the Internet of Things and vehicle-to-everything network. In the future work, we will study the physical layer security techniques to protect the multicast mmWave communication for the entities with high mobility, such as vehicles, drones, and satellites.

REFERENCES

[1] R. W. Heath, N. Gonzalez-Prelcic, S. Rangan, W. Roh, and A. M. Sayeed, "An overview of signal processing techniques for millimeter wave mimo systems," *IEEE Journal of Selected Topics in Signal Processing*, vol. 10, no. 3, pp. 436–453, 2016.

[2] 3GPP, "NR; User Equipment (UE) radio transmission and reception; Part 2: Range 2 Standalone," 3rd Generation Partnership Project (3GPP), Technical Specification (TS) 38.101-2, 04 2020, version 16.3.1.

[3] N. Alliance, "5g white paper," *Next generation mobile networks, white paper*, vol. 1, 2015.

[4] M. Xiao, S. Mumtaz, Y. Huang, L. Dai, Y. Li, M. Matthaiou, G. K. Karagiannidis, E. Björnson, K. Yang, I. Chih-Lin *et al.*, "Millimeter wave communications for future mobile networks," *IEEE Journal on Selected Areas in Communications*, vol. 35, no. 9, pp. 1909–1935, 2017.

[5] Q. Yu, J. Ren, H. Zhou, and W. Zhang, "A cybertwin based network architecture for 6g," in *2020 2nd 6G Wireless Summit (6G SUMMIT)*. IEEE, 2020, pp. 1–5.

[6] M. H. Miraz, M. Ali, P. S. Excell, and R. Picking, "A review on internet of things (iot), internet of everything (ioe) and internet of nano things (iont)," in *2015 Internet Technologies and Applications (ITA)*. IEEE, 2015, pp. 219–224.

[7] S. L. Cotton, W. G. Scanlon, and B. K. Madahar, "Millimeter-wave soldier-to-soldier communications for covert battlefield operations," *IEEE Communications Magazine*, vol. 47, no. 10, pp. 72–81, 2009.

[8] N. Yang, L. Wang, G. Geraci, M. Elkashlan, J. Yuan, and M. Di Renzo, "Safeguarding 5g wireless communication networks using physical layer security," *IEEE Communications Magazine*, vol. 53, no. 4, pp. 20–27, 2015.

[9] Y. Zhu, L. Wang, K.-K. Wong, and R. W. Heath, "Secure communications in millimeter wave ad hoc networks," *IEEE Transactions on Wireless Communications*, vol. 16, no. 5, pp. 3205–3217, 2017.

[10] M. He, J. Ni, Y. He, and N. Zhang, "Low-complexity phased-array physical layer security in millimeter-wave communication for cybertwin-driven v2x applications," *IEEE Transactions on Vehicular Technology*, 2021.

[11] J. Ni, X. Lin, and X. Shen, "Efficient and secure service-oriented authentication supporting network slicing for 5g-enabled iot," *IEEE Journal on Selected Areas in Communications*, vol. 36, no. 3, pp. 644–657, 2018.

[12] W. Trappe, "The challenges facing physical layer security," *IEEE Communications Magazine*, vol. 53, no. 6, pp. 16–20, 2015.

[13] A. Mukherjee, S. A. A. Fakoorian, J. Huang, and A. L. Swindlehurst, "Principles of physical layer security in multiuser wireless networks: A survey," *IEEE Communications Surveys & Tutorials*, vol. 16, no. 3, pp. 1550–1573, 2014.

[14] M. P. Daly and J. T. Bernhard, "Directional modulation technique for phased arrays," *IEEE Transactions on Antennas and Propagation*, vol. 57, no. 9, pp. 2633–2640, 2009.

[15] M. P. Daly, E. L. Daly, and J. T. Bernhard, "Demonstration of directional modulation using a phased array," *IEEE Transactions on Antennas and Propagation*, vol. 58, no. 5, pp. 1545–1550, 2010.

[16] S. Goel and R. Negi, "Guaranteeing secrecy using artificial noise," *IEEE Transactions on Wireless Communications*, vol. 7, no. 6, pp. 2180–2189, 2008.

[17] W. Zhao, S.-H. Lee, and A. Khisti, "Phase-only zero forcing for secure communication with multiple antennas," *IEEE Journal of Selected Topics in Signal Processing*, vol. 10, no. 8, pp. 1334–1345, 2016.

[18] N. Valliappan, A. Lozano, and R. W. Heath, "Antenna subset modulation for secure millimeter-wave wireless communication," *IEEE Transactions on communications*, vol. 61, no. 8, pp. 3231–3245, 2013.

[19] N. N. Alotaibi and K. A. Hamdi, "Switched phased-array transmission architecture for secure millimeter-wave wireless communication," *IEEE Transactions on Communications*, vol. 64, no. 3, pp. 1303–1312, 2016.

[20] Y. Hong, X. Jing, and H. Gao, "Programmable weight phased-array transmission for secure millimeter-wave wireless communications," *IEEE Journal of Selected Topics in Signal Processing*, vol. 12, no. 2, pp. 399–413, 2018.

[21] X. Yao, X. Han, X. Du, and X. Zhou, "A lightweight multicast authentication mechanism for small scale iot applications," *IEEE Sensors Journal*, vol. 13, no. 10, pp. 3693–3701, 2013.

[22] N. Dlodlo, "Adopting the internet of things technologies in environmental management in south africa," 2012.

[23] J. Li, X. Wu, and H. Chen, "Research on mobile digital health system based on internet of things," in *Electrical Power Systems and Computers*. Springer, 2011, pp. 495–502.

[24] X. Shang, R. Zhang, and Y. Chen, "Internet of things (iot) service architecture and its application in e-commerce," *Journal of Electronic Commerce in Organizations (JECO)*, vol. 10, no. 3, pp. 44–55, 2012.

[25] Y. Huang, J. Zhang, and M. Xiao, "Constant envelope hybrid precoding for directional millimeter-wave communications," *IEEE Journal on Selected Areas in Communications*, vol. 36, no. 4, pp. 845–859, 2018.

[26] F. Shu, L. Xu, J. Wang, W. Zhu, and X. Zhou, "Artificial-noise-aided secure multicast precoding for directional modulation systems," *IEEE Transactions on Vehicular Technology*, vol. 67, no. 7, pp. 6658–6662, 2018.

[27] S. E. Nai, W. Ser, Z. L. Yu, and H. Chen, "Beampattern synthesis for linear and planar arrays with antenna selection by convex optimization," *IEEE Transactions on Antennas and Propagation*, vol. 58, no. 12, pp. 3923–3930, 2010.

[28] R. T. Behrens and L. L. Scharf, "Signal processing applications of oblique projection operators," *IEEE Transactions on signal processing*, vol. 42, no. 6, pp. 1413–1424, 1994.

[29] X. Zhang, Z. He, B. Liao, Y. Yang, J. Zhang, and X. Zhang, "Flexible array response control via oblique projection," *IEEE Transactions on Signal Processing*, vol. 67, no. 12, pp. 3126–3139, 2019.

[30] Y.-W. P. Hong, P.-C. Lan, and C.-C. J. Kuo, "Enhancing physical-layer secrecy in multiantenna wireless systems: An overview of signal processing approaches," *IEEE Signal Processing Magazine*, vol. 30, no. 5, pp. 29–40, 2013.

[31] J. Xu, W. Xu, D. W. K. Ng, and A. L. Swindlehurst, "Secure communication for spatially sparse millimeter-wave massive mimo channels via hybrid precoding," *IEEE Transactions on Communications*, vol. 68, no. 2, pp. 887–901, 2020.

[32] M. E. Eltayeb, J. Choi, T. Y. Al-Naffouri, and R. W. Heath, "Enhancing secrecy with multiantenna transmission in millimeter wave vehicular communication systems," *IEEE Transactions on Vehicular Technology*, vol. 66, no. 9, pp. 8139–8151, 2017.

[33] Z. Luo, W. Ma, A. M. So, Y. Ye, and S. Zhang, "Semidefinite relaxation of quadratic optimization problems," *IEEE Signal Processing Magazine*, vol. 27, no. 3, pp. 20–34, 2010.

[34] Z. Pi and F. Khan, "An introduction to millimeter-wave mobile broadband systems," *IEEE Communications Magazine*, vol. 49, no. 6, pp. 101–107, 2011.

[35] B. Fuchs, "Application of convex relaxation to array synthesis problems," *IEEE Transactions on Antennas and Propagation*, vol. 62, no. 2, pp. 634–640, 2013.

[36] B. Liao, C. Guo, L. Huang, Q. Li, and H. C. So, "Robust adaptive beamforming with precise main beam control," *IEEE Transactions on Aerospace and Electronic Systems*, vol. 53, no. 1, pp. 345–356, 2017.

[37] H. Lebret and S. Boyd, "Antenna array pattern synthesis via convex optimization," *IEEE Transactions on Signal Processing*, vol. 45, no. 3, pp. 526–532, 1997.